

Modeling of an airborne wind energy system with a flexible tether model for the optimization of landing trajectories [★]

Jonas Koenemann ^{*,**} Paul Williams ^{*} Soeren Sieberling ^{*}
Moritz Diehl ^{**}

^{*} *Ampyx Power B.V., The Hague, The Netherlands*

^{**} *Dept. of Microsystems Engineering & Dept. of Mathematics,
University of Freiburg, Germany
jonas.koenemann—moritz.diehl@imtek.de,
p.williams—s.sieberling@ampyxpower.com*

Abstract: Autonomous takeoff and landing is a big challenge in the field of airborne wind energy. We propose numerical methods in order to optimize flight trajectories of a tethered aircraft. These flight trajectories yield a baseline for analyzing takeoff or landing performance. In this paper, we optimize for a landing strategy that uses the winch to decelerate the aircraft after touchdown. A complete optimal control formulation with differential algebraic equations for the system dynamics is derived. For avoiding tether collision with the ground, we employ a quasi-static tether model that treats both the tether sag and elasticity. It is a novelty in airborne wind energy trajectory optimization to solve for the tether shape as part of the optimization problem.

© 2017, IFAC (International Federation of Automatic Control) Hosting by Elsevier Ltd. All rights reserved.

Keywords: Tether modeling, Trajectory optimization, Airborne wind energy

1. INTRODUCTION

Airborne wind energy (AWE) is a new technology that aims on harvesting wind energy in higher altitudes than conventional wind turbines while reducing the required amount of material to build the plant. The AWE book by Ahrens et al. (2013) comprises the state-of-the-art of the technology. Ampyx Power B.V. is developing an airborne wind energy system consisting of a rigid wing PowerPlane that is connected to a winch on the ground by a tether. The winch is driven by a motor that also serves as a generator during power generation.

Besides being able to generate power, it is desirable that the system is capable of full autonomous operations which includes autonomous landing in unfavorable wind conditions, and autonomous re-launching when wind conditions improve. There are many concepts that can be considered for launching and landing the PowerPlane. The most promising require as little real-estate on the ground as possible. A key ingredient for achieving this is landing in a short distance to the winch. Landing far from the winch also makes the automation of the re-launching process difficult because the aircraft needs to be pulled back into takeoff position.

Short winch landing is the concept of flying the aircraft over the winch during the approach and using the winch to quickly decelerate the aircraft during touchdown and roll-out. The aircraft will land upwind but close to the

winch, and could be pulled back into takeoff position by the winch and a secondary mechanism. However, the short winch landing maneuver might impose high requirements on the winch because the winch has to quickly switch between reeling in and reeling out during the flyover.

Trajectory optimization is a powerful tool for the analysis of dynamic systems and can be used to study the capabilities of the system, and the feasibility of flight maneuvers given a set of boundary conditions. A model of the underlying system is required in the optimal control formulation. In airborne wind energy, the model of the system consists of an aircraft model, tether model, and a winch model. Flight models are usually developed using polar coordinates to represent the aircraft or kite position (Williams et al., 2007; Fagiano et al., 2012), or using a Cartesian coordinate representation (Gros and Diehl, 2013).

In the field of AWE, numerical optimization of flight trajectories has been presented in several publications. Williams et al. (2008) present models and numerical methods to study the optimal trajectories of cross-wind towing and cross-wind power generation for different wind speeds. Horn et al. (2013) and Licitra et al. (2016) used numerical optimization in order to optimize for periodic power generation cycles. 6-DOF aircraft dynamics were coupled to a straight line tether model in a differential algebraic formulation. The tether is represented by algebraic equations that constrain the distance between the winch and aircraft. They show that with holding patterns, the aircraft can be kept airborne when in low wind conditions, and transition between patterns is possible. Erhard et al. (2016) opti-

[★] Support by the EU via ERC-HIGHWIND (259 166), ITN-TEMPO (607 957), and ITN-AWESCO (642 682) and by DFG in context of the Research Unit FOR 2401.

mized the power orbits of the Skysails kite system and represent the kite position by polar coordinates and the kite orientation by quaternions. Zanon et al. (2014) use an optimal control approach to estimate and control a dual-kite system, and Houska and Diehl (2010) use a robust optimization approach to find control trajectories that are open loop stable.

In the literature, optimal trajectories for AWE systems have employed simple models of the tether which ignore cable sag effects. During the primary phases of operation, this approximation is very good due to the high tension to mass ratio. However, in phases such as launch and land where the tension is significantly smaller, the tether sag becomes important. In practical systems where the tether life must be considered, it is important to maintain the tether from dragging over the ground. Therefore, we seek to go beyond the simplified tether models that have been used in previous work. We present a quasi-static tether model adopted from Williams (2016) which allows to seamlessly integrate the tether model into the optimization problem as algebraic constraint equations.

The structure of the paper is as follows. We first describe a simple flight model and present the proposed tether model in detail which together form the dynamic system model (Section 2). Then, we present the optimal control problem formulation in Section 3 and explain briefly how to solve the optimal control problem with direct transcription methods. We apply the formulation to the problem of short winch landing, stating objective function and constraints, and present the optimized flight trajectories in Section 4.

2. DYNAMIC SYSTEM MODEL

In this section, we describe the mathematical system model that we implemented for optimizing the flight trajectories.

The model describes the dynamical behavior of the system, i.e. the forces and moments acting on the system, as well as the kinematic properties of the system that are expressed by algebraic equations. We therefore use differential algebraic equations (DAE) to formulate the system model. DAEs comprise differential and algebraic equations and have the following implicit form:

$$f^{\text{impl}}(\dot{x}, x, z, u) = 0 \quad (1)$$

where x are the differential variables (states), z the algebraic variables, and u the control variables of the system. Every DAE can be transformed into a semi-explicit form with the following structure:

$$\dot{x} = f(x, z, u) \quad (2a)$$

$$0 = g(x, z, u) \quad (2b)$$

where f are the differential equations and g the algebraic equations stated explicitly.

The models should be simple, but yet represent the behavior of the system for the specific application. For our analysis, which is landing in a non-crosswind scenario, a planar two-dimensional model for the aircraft and the tether is sufficient. However, all models in this paper can be adopted to be used in a three-dimensional scenario.

symbol	value	unit	description
g	9.81	m/s ²	gravitational acceleration
ρ	1.225	kg/m ³	air density
S	3.0	m ²	wing surface area
m	36.6	kg	aircraft's mass
C_{D0}	0.0372		constant drag coefficient
C_{D1}	0.1572	1/rad	linear drag coefficient
C_{D2}	0.6176	1/rad ²	quadratic drag coefficient
C_{L0}	0.5383		constant lift coefficient
C_{L1}	3.9143	1/rad	linear lift coefficient
E	10 ¹¹		elastic modulus of the tether
A	4.91	mm ²	cross section area of the tether
λ^T	0.0046	kg/m	linear density of the tether
d	2.5	mm	diameter of the tether

Table 1. Parameters for the environmental, aircraft, and tether model.

The system in this work consists of aircraft and the tether. Each part of the system is modeled and described in the following sections, followed by a section that describes how to transform the system equations into the form of (2).

2.1 Aircraft flight model

The aircraft dynamics are driven by the sum of forces and moments that are acting on system. In this work, we neglect the pitching moment and assume that the angle of attack can be controlled directly instead of using control surfaces. By limiting the rate of change of the angle of attack we make sure that this a reasonable assumption.

We model the aircraft in flight-path coordinates. The dynamics of the aircraft are expressed in terms of the aircraft's two-dimensional position in north and down direction $p = [p^N, p^D]^T$, the airspeed V , the flight path angle γ , and the angle of attack α . From these terms we can retrieve the ground velocity of the aircraft $v = [v^N, v^D]^T$ by

$$v^N = V \cos(\gamma) + w \quad (3)$$

and

$$v^D = -V \sin(\gamma) \quad (4)$$

where w is the wind speed which is assumed to be constant with altitude in this work.

The forces acting on the aircraft are aerodynamic lift and drag forces, gravity, and the tension force from the tether. The tension force of the tether acting on the body of the aircraft is given by $T = [T^N, T^D]^T$ and will be determined in the next section.

The forces in the direction of flight are given by:

$$m\dot{V} = -\frac{1}{2}\rho V^2 S C_D(\alpha) + T^N \cos(\gamma) - T^D \sin(\gamma) - mg \sin(\gamma) \quad (5)$$

where $C_D(\alpha)$ is the aerodynamic drag coefficient function. The aircraft and environmental parameters are summarized in Table 1.

The orthogonal forces to the flight direction are given by:

$$mV\dot{\gamma} = \frac{1}{2}\rho V^2 S C_L(\alpha) - T^N \sin(\gamma) - T^D \cos(\gamma) - mg \cos(\gamma) \quad (6)$$

where $C_L(\alpha)$ is the aerodynamic lift coefficient function.

The aerodynamic coefficient functions $C_D(\alpha)$ and $C_L(\alpha)$ are aircraft dependent and usually retrieved from CFD

simulations or system identification flights. We use the parameters of the PowerPlane AP2 with 5.5m wingspan that are given in form of lookup tables. In order to ensure a smooth and at least twice differential model, we approximate the lookup tables by first and second order polynomials below the stalling angle of attack. With the parameters from Table 1, the coefficients are given by

$$C_D(\alpha) = C_{D0} + C_{D1}\alpha + C_{D1}\alpha^2 \quad (7)$$

and

$$C_L(\alpha) = C_{L0} + C_{L1}\alpha \quad (8)$$

2.2 Tether model

The most popular flexible tether models in the literature are lumped mass models where the mass points are connected by springs and dampers (Fechner et al., 2015; Williams and Trivailo, 2007). These models have been used for simulating the dynamics system, however they are not suitable in an optimization context because of the high stiffness of the tether. Due to the stiffness, high frequency oscillations will be introduced and therefore a very small time-grid in the discrete optimization problem is required. Furthermore, the state of the system will grow largely with number of mass points, and the initialization of the newton type solver is not trivial. Williams (2010) used a lumped mass model to optimize the orbit of a circularly-towed aircraft-tether system, but neglected the effect of tether elasticity.

Other models are described by differential algebraic equations where the tension forces between the mass points are determined by solving a system of algebraic equations (Zanon et al., 2014). Problems with these model are drifting of the constraint equations, proper initialization of the solver, and how reeling in and out is realized.

For the reason that the presented tether models have difficult dynamic properties in the context of optimization, we instead adopt a quasi-static tether approximation that was presented by Williams (2016). This tether model neglects tether vibrations, but still is capable of representing the tether shape. In the original paper, the quasi-static tether model was used to initialize a dynamic tether model in order to simulate a kite system. We found that this model is very suitable to be used in the optimization context, as the tether is represented only by a few variables and algebraic equations.

The static tether model is represented by $K + 1$ nodes with positions p_k for $k \in [0, K]$ where the first node is at the position of the winch p_0 which is at the origin in this work. Tension forces act along the K links that connect two nodes each (see Fig.1). With a shooting approach, we can calculate the positions of the nodes iteratively starting with the first node with position p_0 :

$$p_{k+1} = p_k + \left(\frac{\|T_k\|}{EA} + 1 \right) \frac{l}{K} \frac{T_k}{\|T_k\|} \quad (9)$$

where T_k is the tension in the k -th link, E the elasticity coefficient of the tether, A the cross section area of the tether, and l the total length of the tether.

The tension forces in the links are calculated iteratively as well. The tension force T_{k+1} in link $k + 1$ depends on the sum of forces that are acting on node k . These

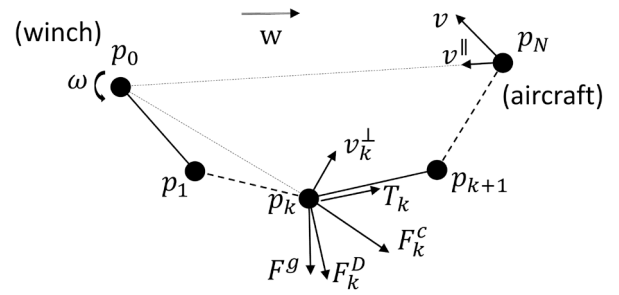


Fig. 1. Representation of the static tether showing the tether nodes (filled circles), links (solid lines), velocity and forces vectors. The dashed lines represent the tether with arbitrary nodes in between, and the thin dashed lines are for a better representation only. The forces acting on the k -th node are the tension force T_k , the gravity force F^g , the drag force F_k^D , and the centripetal force F_k^c . Centripetal and drag forces depend on the node velocity v_k and the aircraft velocity v . The node positions p_k and tension force T_k are calculated iteratively starting from the winch position p_0 and tension at the winch T_0 .

forces are the tension force of the previous link, the centripetal force F_k^c , gravity, and the drag force F_k^D . Figure 1 illustrates the forces on the tether. With these forces we can iteratively calculate the tension force for all links $k = 1 \dots K - 1$ starting with the tension force at the winch $T_0 = [T_0^N, T_0^D]^T$

$$T_{k+1} = T_k + F_k^c - [0, mg]^T - F_k^D \quad (10)$$

and where $m = \frac{l}{K} \lambda^T$ is the mass of one link with the linear density of the tether λ^T . The centripetal and drag forces are derived in the following.

Velocity model The tether is approximated as a rigid body while the tip of the tether has to match the velocity of the aircraft v . The aircraft's velocity can be decomposed into an angular component ω and tangential component $v^||$ (see Fig. 1). With the tangential direction of the aircraft with respect to the winch given by

$$\hat{p} = \frac{p - p_0}{\|p - p_0\|} \quad (11)$$

we can get the tangential velocity by

$$v^|| = \langle \hat{p}, v \rangle \hat{p} \quad (12)$$

where $\langle \cdot, \cdot \rangle$ designates the dot product.

The angular component of the aircraft's velocity is given by:

$$\omega = \frac{\|v - v^||\|}{\|p - p_0\|} \quad (13)$$

For the tether nodes, we decompose the velocities into a orthogonal and tangential part. Using the rigid-body assumption, the orthogonal velocity is known to be

$$v_k^perp = \omega \begin{bmatrix} 0 & -1 \\ 1 & 0 \end{bmatrix} (p_k - p_0) \quad (14)$$

while the tangential part is assumed to be equal to the aircraft's tangential velocity, so $v_k^|| = v^||$.

Centripetal force and drag model With these quantities we can now calculate the centripetal force:

$$F_k^c = m\omega^2(p_k - p_0) \quad (15)$$

It is left to describe the drag model of the tether. Drag is acting on each link of the tether and depends on the relative velocity of the link in the airflow. From the components of the node velocity, we can get the relative velocity to the wind speed w by

$$v_k^a = v_k^\perp + v_k^\parallel - [w, 0]^\top \quad (16)$$

We employ a cross-flow model of tether drag. The tangential direction is given by the direction of the tension force $\hat{T}_k = \frac{T_k}{\|T_k\|}$, so we get the part of the cross-flow velocity by:

$$v_k^\times = v_k^a - \langle v_k^a, \hat{T}_k \rangle \hat{T}_k \quad (17)$$

Finally, the drag force is determined by:

$$F_k^D = -\frac{1}{2}C_D^c \frac{l}{K} d\rho \|v_k^\times\| v_k^\times \quad (18)$$

where the tether is assumed cylindric with a drag coefficient of $C_D^c = 1.2$, and the aerodynamic area of the link is determined by the length of the tether l , the number of links K , and the tether diameter d .

To summarize the tether model, with (9) and (10) we can calculate the tether shape represented by the positions of the $K + 1$ nodes, and the tension forces in the K links. The position of the last node of the tether $p_K = [p_K^N, p_K^D]^\top$ only depends on the tension force in the first link $T_0 = [T_0^N, T_0^D]^\top$ and the tether length l . The tension acting on the aircraft is given by the tension in the last link, but in the other direction, so $T^N = -T_{K-1}^N$ and $T^D = -T_{K-1}^D$.

We can solve the tether shape by an root finding problem with two variables for the tension in the first link T_0^N and T_0^D , and two equations. The solver will determine the required tension force to satisfy the equations. This optimization problem can be seamlessly solved together with the system model in a DAE formulation described in the next section.

In this work we use the parameters of the 2.5mm Dyneema tether of the PowerPlane AP2. All tether parameter values are listed in Table 1.

2.3 System equations

In this section we collect the model equations from the previous section and bring it in the form of the semi-explicit DAE of (2). The state of the system consisting of the aircraft and tether model described in Sections 2.1 and 2.2 can be described by the state variables for north position p_N , down position p_D , airspeed V , flight path angle γ , angle of attack α , and tether length l . The algebraic variables that appear in the tether model and that need to be solved for are the tension on the winch in north- and down-direction T_0^N, T_0^D .

However, we introduce additional variables for the system for two main reasons. If a DAE solver is used, one can easily introduce meaningful additional algebraic variables determined by algebraic equations. Here, we introduce a tension variable T that represents the magnitude of the tension in the tether. Furthermore, we want to ensure the generated solutions maintain smooth, realistic variations in the controlled outputs. Therefore, a second set of

variables is introduced in order to use derivatives of variables in the problem formulation. These variables are determined by simple differential equations. Here, we introduce variables for the tether length rate \dot{l} , the tether length acceleration \ddot{l} , the tension rate \dot{T} , and the tension acceleration \ddot{T} .

The complete state of the system is given by

$$x = [p^N, p^D, V, \gamma, \alpha, l, \dot{l}, T, \dot{T}]^\top \quad (19)$$

while the algebraic variables are

$$z = [T_0^N, T_0^D, \ddot{T}]^\top \quad (20)$$

and the control variables are

$$u = [\dot{\alpha}, \ddot{l}]^\top \quad (21)$$

The differential equations as in (2a) relate the state variables, control variables, and the algebraic variables to the derivatives of the state variables:

$$\dot{x} = \begin{bmatrix} V \cos(\gamma) + w \\ -V \sin(\gamma) \\ \text{from (5)} \\ \text{from (6)} \\ \dot{\alpha} \\ \dot{l} \\ \ddot{l} \\ \dot{T} \\ \ddot{T} \end{bmatrix} \quad (22)$$

The algebraic equation in form of (2b) is given by

$$0 = \begin{bmatrix} p^N - p_K^N(x, u, T_0^N, T_0^D) \\ p^D - p_K^D(x, u, T_0^N, T_0^D) \\ \|[T_0^N, T_0^D]\|^2 - T^2 \end{bmatrix} \quad (23)$$

where the first two rows determine the tension forces acting on the winch in north and down direction T_0^N, T_0^D , and the third row determines the tension magnitude T .

3. OPTIMAL CONTROL PROBLEM FORMULATION

An optimal control problem is an optimization problem to minimize a cost function defined on the state, control, and algebraic variables of the system integrated over a finite time horizon. The system dynamics have to be satisfied and appear as constraint equations in the optimal control problem formulation. We use a continuous time formulation that will be discretized in time using direct transcription methods.

3.1 Continuous time optimal control problem

The general continuous time formulation of the optimal control problem used in this work is the following:

$$\begin{aligned} & \underset{X, Z, U, T}{\text{minimize}} && \int_0^{\mathcal{T}} c(x(t), z(t), u(t)) \, dt \\ & \text{subject to} && \dot{x}(t) = f(x(t), z(t), u(t)) && \text{dynamic equations} \\ & && 0 = g(x(t), z(t), u(t)) && \text{algebraic equations} \\ & && h(x(t), z(t), u(t)) \leq 0 && \text{path constraints} \\ & && h_0(x(0)) \leq 0 && \text{initial constraints} \\ & && h_{\mathcal{T}}(x(\mathcal{T})) \leq 0 && \text{terminal constraints} \\ & && && \text{for } t \in [0, \mathcal{T}] \end{aligned}$$

where X, Z, U are the state, algebraic, and control variables along the flight trajectory, and $c(x, z, u)$ the cost function. In the continuous time formulation, the optimization variables are actually functions that define the system variables x, z, u for the whole interval $t \in [0, \mathcal{T}]$. This is indicated by the capitalized symbols. We also define the final time \mathcal{T} as an optimization variable so that the optimal flight time is determined by the optimizer.

3.2 Direct transcription method

We use direct methods in order to transcribe the continuous time formulation into a discrete time formulation. The resulting non-linear program can then be solved by standard state-of-the-art non-linear programming solvers. The advantage of the direct collocation method is that it is particularly suitable for solving very non-linear, long-horizon problems. It has been successfully used by Horn et al. (2013) in order to solve long-horizon power generation cycles. For an overview of trajectory optimization methods we refer to Betts (2010).

In order to integrate the system dynamics, we use a Radau collocation scheme which is an implicit integration method suitable for optimal control problems with a DAE system model (Biegler, 2007). The dynamic equations are directly integrated into the optimization problem and are solved by the non-linear programming solver together with the boundary conditions as in the formulation of Horn et al. (2013). We choose the order of the collocation scheme to be two, and the number of intervals for the time-discretization of the problem to be 30.

After transcribing the optimal control problem to a non-linear program, we use the symbolic framework CasADi to implement the optimization problem (Andersson, 2013). CasADi provides a MATLAB interface to model and formulate the non-linear optimization problem (MATLAB, 2014). Using the symbolic implementation, it can automatically generate necessary derivatives like the Jacobian of the constraints function and the Hessian of the Lagrange function that are needed in the Newton iteration. Derivatives are calculated with algorithmic differentiation. In this work we use the interface of CasADi to Ipopt by Wächter and Biegler (2006), a software package for solving large-scale non-linear optimization problems with the interior point method. We keep all options of the solver at default settings.

4. OPTIMAL CONTROL OF A SHORT WINCH LANDING

As the aircraft is connected to the winch by the tether, the winch can be used to quickly decelerate the aircraft, and a landing within a short distance to the winch can be achieved. The landing starts downwind of the winch with the approach of the aircraft. The aircraft will fly over the winch and touches down upwind of the winch, while tension force in the tether brakes the aircraft. In this work, we optimize the flight trajectory from the moment when the aircraft is downwind of the winch and has 20 meters altitude, until the moment when the aircraft is upwind, close to the ground, and the tension force in the tether is high.

In the following subsections, we will propose a formulation for the cost function (Section 4.1) and boundary conditions (Section 4.2). This formulation is for one flight scenario only but can easily be adapted to consider different flight criteria. We will briefly explain how the solver was initialized (Section 4.3) and present the resulting flight trajectory in Section 4.4.

4.1 Cost function

The cost function in the optimal control problem is to minimize the total squared accelerations on the aircraft along the flight trajectory. Minimizing the total accelerations generally leads to a smooth flight trajectory. The total forces on the aircraft are described in (5) and (6). In the cost function however, we leave out the forces from the tether tension because we want to decelerate the aircraft using the tether during landing, and therefore not penalize tension forces too much.

We add small regularization terms to penalize control inputs, algebraic variables, and tension forces. The complete cost function is given by

$$c(x, z, u) = \left(-\frac{1}{2}\rho V^2 SC_D(\alpha) - mg \sin(\gamma)\right)^2 + \left(\frac{1}{2}\rho V^2 SC_L(\alpha) - mg \cos(\gamma)\right)^2 + 10^{-8}(u^\top u) + 10^{-8}(z^\top z) + 10^{-3}T^2 \quad (24)$$

4.2 Boundary conditions

When optimizing flight trajectories, the system has to satisfy a couple of constraints so that the resulting trajectory is feasible, i.e. the requirements on aircraft and winch can be met. We also have to make sure that the solution is valid for our model assumptions, e.g. the approximation of the aerodynamic coefficients is only valid for a specific range of angle of attack. Because all quantities that we want to constrain are actually variables in our problem formulation, we can easily implement path constraints as bounds on the variables. In this work we use the following constraints:

- Angle of attack: $-5.7^\circ \leq \alpha \leq 17.2^\circ$
- Rate of angle of attack: $-11.5^\circ \text{s}^{-1} \leq \dot{\alpha} \leq 11.5^\circ \text{s}^{-1}$
- Airspeed: $13 \frac{\text{m}}{\text{s}} \leq V \leq 40 \frac{\text{m}}{\text{s}}$
- Tether length: $1\text{m} \leq l \leq 200\text{m}$
- Tether length rate: $-25 \frac{\text{m}}{\text{s}} \leq \dot{l} \leq 25 \frac{\text{m}}{\text{s}}$
- Tether length acceleration: $-50 \frac{\text{m}}{\text{s}^2} \leq \ddot{l} \leq 50 \frac{\text{m}}{\text{s}^2}$
- Tension magnitude: $8\text{N} \leq T \leq 1000\text{N}$
- Tension rate: $-1000 \frac{\text{N}}{\text{s}} \leq \dot{T} \leq 1000 \frac{\text{N}}{\text{s}}$
- Tension acceleration: $-3000 \frac{\text{N}}{\text{s}^2} \leq \ddot{T} \leq 3000 \frac{\text{N}}{\text{s}^2}$
- Tether is not touching the ground: $-200\text{N} \leq T_0^D \leq 0$

Note that the constraint forcing the tether not to touch the ground is realized by constraining the tension on the winch to be in upward direction. We limit tether rate and acceleration to comply with winch specifications, and we limit the tension rate and acceleration to get a smooth transition from low to high tension.

We further implement initial and terminal constraints to define the beginning and the end of the flight trajectory.

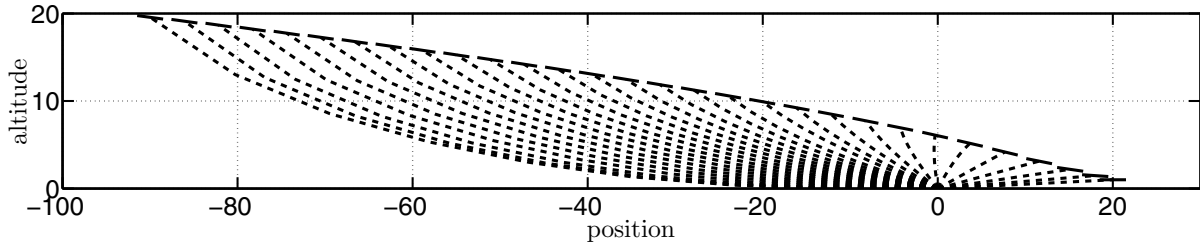


Fig. 2. Optimal flight trajectory for the short winch landing. The position of the aircraft and the pitch angle are indicated by the black bars. The tether shown as the dotted lines does not collide with the ground. The trajectory of the aircraft starts at 94m downwind position. A landing at 20m upwind position with a nearly constant flight path angle is achieved.

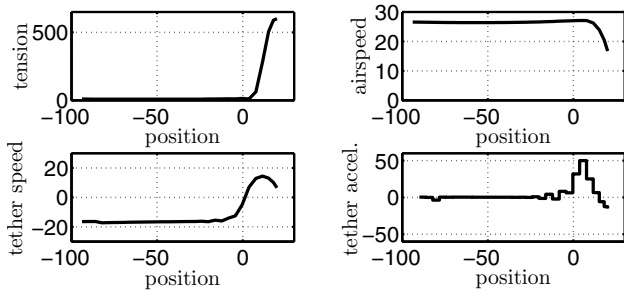


Fig. 3. Evolution of tension, airspeed, tether speed, and tether acceleration during the flight trajectory. While the aircraft is flying over the winch, the winch switches from reeling in to reeling out, and the tension in the tether increases until the desired tension and airspeed for landing is achieved.

Here, the start of the optimized trajectory begins when the aircraft has 20m altitude and is at least 20m downwind of the winch, implemented as the bounds on initial state:

- initial altitude 20m: $p^D(0) = -20\text{m}$
- Initial north position $-\infty \leq p^N(0) \leq -20\text{m}$

The flight should end at 20m up wind position and meet the following terminal constraints:

- Final altitude 1m: $p^D(\mathcal{T}) = -1\text{m}$
- Final north position $p^N(\mathcal{T}) = 20\text{m}$
- Final tension: $T(\mathcal{T}) \geq T^{\text{des}}$
- Final tension rate: $T(\mathcal{T}) = 0 \frac{\text{N}}{\text{s}}$
- Final sink rate: $0 \leq -V(\mathcal{T}) \sin(\gamma(\mathcal{T})) \leq 2 \frac{\text{m}}{\text{s}}$
- Final positive pitch angle: $\alpha(\mathcal{T}) + \gamma(\mathcal{T}) \geq 0^\circ$

where T^{des} is a parameter to specify the desired tension at the end of the trajectory. For the solution of the short winch landing problem we set $T^{\text{des}} = 600\text{N}$ but for initialization purposes this parameter is varied (see Section 4.3). The trajectory should end with no change in tension force so that we can assume a constant tension after touchdown. In a practical implementation, one has to design a winch controller that keeps the tether tension constant during the roll-out and drops off the tension shortly before full-stop.

We end the flight at 1m altitude of the center of mass because the aircraft might have an undercarriage. Ending the trajectory at 0m would make the formulation infeasible because infinite tension forces would be required to have no tether sag.

4.3 Initialization

As the optimization problem is non-linear, we need to provide a reasonable initial guess in order to prevent excessive computation time and convergence to local minima. We observed that high tensions on the tether at the end of the flight trajectory pose difficulties for the solver. For that reason we solve a simpler problem first, with a low for the final tension T^{des} . Then we use the solution of the simpler problem to initialize the more difficult problem. Using this homotopy strategy, we gradually increase the final tension force until the high desired tension force is reached.

The low tension problem can be solved with simple initial guesses for the variables. We use a linear assignment of the position variables between the first and the last position, a linear assignment for the tether length, and constant values for all other variables.

4.4 Short winch landing solution

The optimized flight trajectory for the short winch landing problem is shown in Fig. 2. The optimization was performed with a wind-speed of $10 \frac{\text{m}}{\text{s}}$ constant with altitude. The aircraft starts with an altitude of 20m at about 94m downwind and passes the winch at a height of 7m, so the inertial glide-slope during the approach is about -4.5° . We can see that the tether has more slack in the beginning of the trajectory and less slack in the last part, but the tether is not in contact with the ground.

The plots in Fig. 3 show the airspeed, magnitude of the tension force, tether speed, and tether acceleration during the flight. The tether tension is minimal during the first part of the trajectory but increases after the aircraft passed the winch. The airspeed is relatively constant until the aircraft is decelerated from the tether tension.

The winch switches from reeling in to reeling out just when the aircraft passes the winch. The reeling speed is well within the specified limits of $25 \frac{\text{m}}{\text{s}}$. However, the tether acceleration limit of $50 \frac{\text{m}}{\text{s}^2}$ is getting hit when the winch switches from reeling in to reeling out. This should be considered in a winch design.

5. CONCLUSION

We showed that optimal control can be used to optimize complex flight trajectories of a tethered aircraft, even if

an advanced tether model representing elasticity and sag is used. We found a flight trajectory for the short winch landing maneuver that satisfies all boundary conditions and can be flown with a real aircraft. While this is an example trajectory, with the presented problem formulation, important design parameters for the aircraft and the winch can be determined by varying limits on the variables. The landing performance can be tested for different landing distances, final tension force, or wind speeds. Because of the high requirements on the winch during the short winch landing maneuver, further modeling of the winch mechanics and electronics could be considered in future work.

REFERENCES

- Ahrens, U., Diehl, M., and Schmehl, R. (2013). *Airborne wind energy*. Springer Science & Business Media.
- Andersson, J. (2013). *A General-Purpose Software Framework for Dynamic Optimization*. PhD thesis, Arenberg Doctoral School, KU Leuven, Department of Electrical Engineering (ESAT/SCD) and Optimization in Engineering Center, Kasteelpark Arenberg 10, 3001-Heverlee, Belgium.
- Betts, J.T. (2010). *Practical methods for optimal control and estimation using nonlinear programming*, volume 19. Siam.
- Biegler, L.T. (2007). An overview of simultaneous strategies for dynamic optimization. *Chemical Engineering and Processing: Process Intensification*, 46(11), 1043–1053.
- Erhard, M., Horn, G., and Diehl, M. (2016). A quaternion-based model for optimal control of an airborne wind energy system. *ZAMM-Journal of Applied Mathematics and Mechanics/Zeitschrift für Angewandte Mathematik und Mechanik*.
- Fagiano, L., Milanese, M., and Piga, D. (2012). Optimization of airborne wind energy generators. *International Journal of robust and nonlinear control*, 22(18), 2055–2083.
- Fechner, U., van der Vlugt, R., Schreuder, E., and Schmehl, R. (2015). Dynamic model of a pumping kite power system. *Renewable Energy*, 83, 705–716.
- Gros, S. and Diehl, M. (2013). Modeling of airborne wind energy systems in natural coordinates. In *Airborne wind energy*, 181–203. Springer.
- Horn, G., Gros, S., and Diehl, M. (2013). Numerical trajectory optimization for airborne wind energy systems described by high fidelity aircraft models. In *Airborne wind energy*, 205–218. Springer.
- Houska, B. and Diehl, M. (2010). Robustness and stability optimization of power generating kite systems in a periodic pumping mode. In *2010 IEEE International Conference on Control Applications*, 2172–2177. IEEE.
- Licitra, G., Siberling, S., Engelen, S., Williams, P., Ruiterkamp, R., and Diehl, M. (2016). Optimal control for minimizing power consumption during holding patterns for airborne wind energy pumping system. In *European Control Conference*.
- MATLAB (2014). *MATLAB version 2014a*. The Mathworks, Inc., Natick, Massachusetts.
- Wächter, A. and Biegler, L.T. (2006). On the implementation of an interior-point filter line-search algorithm for large-scale nonlinear programming. *Mathematical Programming*, 106(1), 25–57.
- Williams, P. (2010). Optimization of circularly towed cable system in crosswind. *Journal of guidance, control, and dynamics*, 33(4), 1251–1263.
- Williams, P. (2016). Cable modeling approximations for rapid simulation. *Journal of guidance, control, and dynamics (submitted)*.
- Williams, P., Lansdorp, B., and Ockels, W. (2007). Modeling and control of a kite on a variable length flexible inelastic tether. In *AIAA Guidance, navigation and control conference*.
- Williams, P., Lansdorp, B., and Ockels, W. (2008). Optimal crosswind towing and power generation with tethered kites. *Journal of guidance, control, and dynamics*, 31(1), 81–93.
- Williams, P. and Trivailo, P. (2007). Dynamics of circularly towed aerial cable systems, part i: optimal configurations and their stability. *Journal of guidance, control, and dynamics*, 30(3), 753–765.
- Zanon, M., Horn, G., Gros, S., and Diehl, M. (2014). Control of dual-airfoil airborne wind energy systems based on nonlinear mpc and mhe. In *Control Conference (ECC), 2014 European*, 1801–1806. IEEE.